Calculating NMR Chemical Shifts in Solvated Systems

Leah B. Casabianca

Department of Chemistry, Clemson University, Clemson, SC, USA

Abstract

The NMR chemical shift is extremely sensitive to molecular geometry, hydrogen bonding, solvent, temperature, pH, and concentration. Calculated magnetic shielding constants, converted to chemical shifts, can be valuable aids in NMR peak assignment and can also give detailed information about molecular geometry and intermolecular effects. Calculating chemical shifts in solution is complicated by the need to include solvent effects and conformational averaging. Here we review the current state of NMR chemical shift calculations in solution, beginning with an introduction to the theory of calculating magnetic shielding in general, then covering methods for inclusion of solvent effects and conformational averaging, and finally discussing examples of applications using calculated chemical shifts to gain detailed structural information.

Keywords: NMR, ^{1}H, ^{13}C, ^{15}N, chemical shift, computation, solvent

1. Introduction

The NMR chemical shift is the easiest NMR parameter to measure, and contains a wealth of information. The chemical shift is extremely sensitive to the electronic environment surrounding the nucleus in question, and is influenced by intramolecular and intermolecular effects including for example molecular geometry and hydrogen bond distance. The chemical shift therefore contains extremely specific details regarding the structure of molecules and their environment, and it is up to us as spectroscopists to obtain and interpret that information.

Calculated chemical shifts, using density functional or *ab initio* methods, can provide insight into the many factors that influence the NMR chemical shift. As available computing power increases, calculated chemical shifts are becoming readily available for many nuclei in large molecules with greater accuracy. Calculated chemical shifts can be used for peak assignment, which is the first step in structure determination of small molecules, natural products, and proteins by NMR. Beyond peak assignment, comparison of experimental and calculated chemical shifts can be used to understand both the specific geometry of the molecule in question and how it interacts with neighboring molecules. These intramolecular and intermolecular effects on NMR chemical shift have been discussed in several excellent reviews on NMR shielding calculations.[1-5]

In the present review, we focus on chemical shift calculations in solution. While solid-state and gas phase NMR can give more information than solution-state NMR, these experiments require specialized equipment and knowledge to extract this information. Solution-state NMR, on the other hand, is used daily for rapid, facile structure determination by specialists and non-specialists alike. Modeling NMR chemical shifts in solution, however, presents additional challenges compared to calculations of NMR chemical shifts for solid-state structures. First, the effects of the solvent need to be considered.[6,7] This can be done by modeling the solvent implicitly as a dielectric, or by addition of explicit solvent molecules. In either case, both the accuracy and computational efficiency of the solvent model need to be considered. The other difficulty in predicting NMR chemical shifts in solution is that molecules in solution are dynamic and the observed chemical shift is a weighted average of all accessible low-energy structures. Taking into account all of the accessible structures of a molecule in solution can easily add to the computational cost.

Being an electronic property, magnetic shielding is extremely sensitive to the environment surrounding the nucleus. Although this is what makes the chemical shift such a powerful observable, this strong dependence of chemical shift on molecular structure and environment

makes chemical shifts in solution difficult to predict. Any chemist who has used NMR knows that the observed chemical shift depends on a variety of factors including the solvent, concentration, temperature, pH, etc. Accounting for all of these effects in a computational method can be difficult, but can also provide a rigorous test of the computational method itself.

This review is organized as follows: In the rest of this section, we provide an overview of computational chemistry methods and an introduction to the calculation of NMR shielding tensors. We then discuss strategies for overcoming the two main challenges of predicting NMR chemical shifts in solution: incorporation of solvent effects and conformational averaging. We conclude by discussing several applications of using calculated chemical shifts to solve problems in solution-state NMR. We hope that we can convince the reader that although calculating NMR chemical shifts in the solution state is complicated, useful information can be gained from these calculations, and that chemical shift calculation can be a valuable tool in molecular structure determination.

1.1 Overview of Computational Chemistry

Computational chemistry falls into two categories: molecular mechanics methods and quantum chemical methods. Molecular mechanics is based on the laws of classical physics, while, as the name suggests, quantum mechanical methods utilize the laws of quantum mechanics. Molecular mechanics considers each atom as a single entity (coarse-grained methods consider groups of atoms, such as a CH_3 or CH_2 group, as a single entity) and requires bonds between atoms to be defined. Quantum mechanics, on the other hand, considers nuclei and electrons separately, and defines a bond only by proximity of two nuclei and increased electron density between them. Molecular mechanics is computationally less expensive, and as such is generally used to model large, biological systems, and for molecular dynamics (MD) simulations, but usually cannot model bond formation and breaking. There are some specialized molecular mechanics methods that do allow for bond formation and breaking,[8] but these are outside the scope of this review. In the context of calculating NMR chemical shifts, quantum chemistry methods must be used to describe the interaction between the nucleus and its surrounding electrons, but molecular mechanics methods are often used to incorporate solvent effects or to describe the dynamics of the system for conformational averaging.

$$V(r)_{bond} = K_b(b - b_0)^2$$

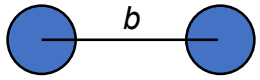

$$V(r)_{angle} = K_\theta(\theta - \theta_0)^2$$

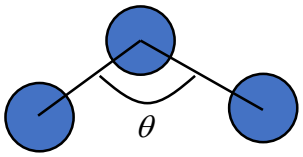

$$V(r)_{dihedrals} = K_\chi[1 + \cos(n\chi - \sigma)]$$

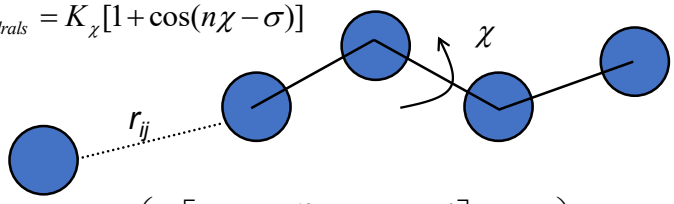

$$V(r)_{external} = \sum_{\substack{nonbonded \\ atom\_pairs}} \left(\varepsilon_{ij} \left[\left(\frac{R_{\min,ij}}{r_{ij}} \right)^{12} - \left(\frac{R_{\min,ij}}{r_{ij}} \right)^{6} \right] + \frac{q_i q_j}{\varepsilon_D r_{ij}} \right)$$

Figure 1. Illustration of parameters that define a molecular mechanics force field. Equilibrium values and force constants that describe bonds, angles, dihedral angles, and parameters describing non-bonded interactions (among others) comprise an empirical molecular mechanics force field.[9]

As shown in Figure 1, molecular mechanics methods are based on force fields that consist of equilibrium bond lengths, angles, dihedral angles, force constants for each of these parameters, and van der Waals parameters for each distinct type of atom. Bonds between atoms are essentially modeled as springs by assuming a quadratic potential; bond angles are also given a quadratic potential. Dihedral angles are assigned a periodic potential and van der Waals interactions between non-bonded atoms are modeled with a Lennard-Jones or similar potential. The energy of the system is then computed as a sum of all bond, angle, dihedral, van der Waals, and electrostatic energy contributions. Molecular mechanics methods are frequently used in molecular dynamics simulations. In classical MD simulations, all atoms in the system are randomly assigned initial velocities at the given temperature, the forces on each atom are calculated, and the system is propagated through time using Newton's equations of motion. Classical molecular mechanics methods may seem naïve compared to the quantum mechanical methods described below, but they have an indispensable role in modeling systems that are too large to model quantum mechanically, and have allowed the study of time-dependent processes, as well as conformational averaging as a function of time.

Among quantum calculation methods, there are various levels of theory. In general, as the complexity of the computational method increases, both the accuracy and computational cost tend to increase, although this is not always strictly the case. The simplest quantum mechanical method is the Hartree-Fock (HF) method[10], which minimizes the energy variationally using a single Slater determinant. HF is the starting point for many higher-level methods, but HF is not often chosen as the final method for calculation because it does not correctly model electron correlation – the time-dependent interaction between electrons. Post-Hartree-Fock methods, including configuration interaction[11] (CI), coupled-cluster theory[12] (CC), and Møller-Plesset perturbation theory[13] (MPPT), correct for this deficiency with additional computational cost.

As an alternative to more expensive post-Hartree-Fock methods, Density Functional Theory (DFT) is a method that models electron correlation at a reduced computational cost.[14] DFT is based on the Kohn-Sham theorem[15] which states that the energy of a system is uniquely determined by a functional of the electron density. A functional is a function of a function – the electron density being a function of nuclear coordinates. The main challenge in DFT is that the functional that describes the energy as a function of electron density is not known, and much research has gone into developing approximate functionals that give accurate results. The reader may be familiar with local density approximation (LDA) or "local" functionals such as VWN[16]; gradient corrected (GGA) functionals: PW91[17-20], LYP[21], or B88[22]; meta-GGA functionals: M06-L[23]; or hybrid functionals including B3LYP.[24,21] DFT has become a popular and powerful method for quantum mechanical calculations because DFT calculations can rival the accuracy of post-HF methods with a computational cost comparable to that of HF. The disadvantage of DFT is that there is no way to systematically improve the results – in other words, there is no way to predict whether one functional or another will give the best results for a particular calculation on a particular system, or for that matter to tell whether the answer given by one functional is more accurate than that given by another functional without comparing to experimental results.

A quantum mechanical calculation also requires a definition of a basis set. Basis sets are mathematical functions used to represent electronic orbitals. A hydrogen 1s orbital has the form of a Slater-type orbital ($\psi_{1s} = Ne^{-\alpha r}$) but Gaussian-type functions ($\psi_G = Ne^{-\alpha r^2}$) are easier to work with computationally (the product of two Gaussians is another Gaussian centered on the line connecting the two original Gaussians). What is typically done is fit a Slater-type atomic orbital

with a linear combination of several Gaussians.[25] Molecular orbitals are constructed as a linear combination of atomic orbitals, and during a calculation the coefficients in the linear combinations are varied to find the molecular orbitals that when occupied lead to the minimum energy. (The linear combination of Gaussian functions that are fit to a Slater-type function does not change during the course of the calculation.) The number of basis functions is often larger than the total number of atomic orbitals – for example, it is common to use two (a split-valence or double-zeta basis set) or three (triple-zeta) basis functions to represent each valence orbital. A larger basis set allows electrons more freedom to find a lower-energy configuration, but requires more computational time. Diffuse and polarization functions (allowing the molecular orbitals more flexibility to change shape) can also be added to a basis set to give the electrons even more flexibility. For calculations of periodic systems in solids, plane-wave basis functions are used instead of local basis functions, providing the foundation of the Gauge Including Projected Augmented Wave (GIPAW) approach[26] for calculating NMR chemical shifts.

In a quantum mechanical calculation, the Born-Oppenheimer approximation is applied, and the energy is calculated at a fixed nuclear geometry. Because the NMR chemical shift is extremely sensitive to geometry, it is important to calculate the NMR shielding at the "correct" geometry. In order to find a reasonable molecular structure, geometry optimizations may be carried out using quantum mechanical methods. Various algorithms are used to find the optimized geometry corresponding to an energy minimum, and these algorithms essentially consist of calculating an energy at the starting geometry, moving the atoms, and calculating the energy at this new geometry, continuing until a minimum energy configuration of the nuclei has been found. It is generally good practice to perform a geometry optimization before calculating NMR shielding constants. Zero-point vibrational corrections can also be significant for calculation of magnetic shielding tensors, and so should also be taken into account when possible.[27-29] Keep in mind that geometry optimizations find only the closest ***local*** minimum according to the energy calculated at a particular model chemistry, and do not take into account conformational averaging. Alternatively, it is also possible to calculate the NMR shielding at a deliberately non-optimized geometry. For example, one can vary a bond length or torsion angle to examine how shielding changes as a function of molecular geometry.[30]

Although molecular dynamics is usually calculated using classical force field methods, another method for performing dynamics is *ab initio* molecular dynamics (AIMD). In AIMD, sometimes called Car-Parrinello molecular dynamics[31] (CPMD), instead of using an empirically-determined force field to calculate the forces on each atom, forces are calculated at each step in the simulation using *ab initio* or density functional methods. This approach uses the Born-Oppenheimer approximation, and nuclei are treated classically so that the system can propagate through time using Newton's equations of motion. Advantages of CPMD over classical MD are that the results do not depend on a pre-defined force field (although if DFT is used for the force calculations, they depend on a pre-defined density functional which also introduces an approximation), and AIMD can handle bond breaking and formation, and changes in charge distribution throughout the simulation. As can be expected, because AIMD requires an *ab initio* calculation at each step in the trajectory, these calculations can take significantly more computational time and resources than classical MD simulations, and consequently are restricted to much shorter timescales than classical MD[32].

1.2 Calculation of NMR Shielding

For detailed discussions on calculation of NMR parameters, including shielding, the reader is referred to several books and reviews.[33-35] In order to calculate nuclear magnetic shielding, we need to calculate the current that is generated by electrons in an atom or molecule in the presence

of an external magnetic field. Nuclear magnetic shielding is defined as the second derivative of the energy with respect to the magnetic moment of the nucleus (μ) and the external magnetic field (B):

$$\sigma_{ab} = \left(\frac{\partial^2 E}{\partial \mu_a \partial B_b}\right)_{\mu,B=0} \tag{1}$$

Where the subscripts a and b indicate that the shielding is not a scalar value but a rank-2 tensor:

$$\sigma = \begin{pmatrix} \sigma_{xx} & \sigma_{yx} & \sigma_{zx} \\ \sigma_{xy} & \sigma_{yy} & \sigma_{zy} \\ \sigma_{xz} & \sigma_{yz} & \sigma_{zz} \end{pmatrix} \tag{2}$$

Where σ_{ij} indicates the shielding in the i-direction when the magnetic field is oriented in the j-direction. In solution-state NMR, however, a single value of chemical shift is typically observed for each nucleus. This is because rapid molecular tumbling averages out the orientation-dependent part of the shielding tensor and only the isotropic value is observed. Single-crystal NMR experiments in the solid state are required to obtain all nine values of the shielding tensor experimentally. The shielding tensor can be diagonalized, leading to the three principal tensor components:

$$\sigma = \begin{pmatrix} \sigma_{xx} & 0 & 0 \\ 0 & \sigma_{yy} & 0 \\ 0 & 0 & \sigma_{zz} \end{pmatrix} \tag{3}$$

These three principal components can be determined experimentally from a solid-state NMR powder pattern. The isotropic value of the shielding is the average of these three principal component values:

$$\sigma_{iso} = \frac{\sigma_{11} + \sigma_{22} + \sigma_{33}}{3} \tag{4}$$

The isotropic value is the value that is observed in solution-state NMR. It is important to note that quantum chemical calculations can provide not only the full nine components of the shielding tensor, but the orientation of this tensor with respect to the molecular frame as well.

Since the changes in electron density that are induced by the presence of an external magnetic field are small for the field strengths used in NMR, we can use perturbation theory to calculate the nuclear magnetic shielding. The presence of a magnetic field introduces an additional term in the Hamiltonian,

$$\hat{H} = \left(\frac{1}{2m}\right)[-i\hbar\nabla]^2 + V \tag{5}$$

such that the Hamiltonian in the presence of an external magnetic field is:

$$\hat{H} = \left(\frac{1}{2m}\right)\left[-i\hbar\nabla - \left(\frac{e}{c}\right)A\right]^2 + V \tag{6}$$

where e is the charge on the electron, c is the speed of light, and A is the magnetic vector potential, which has been defined such that:

$$B = \nabla \times A \tag{7}$$

In the presence of a nuclear magnetic moment, A can be written as the sum of two terms. The first term is the vector potential due to the external magnetic field and the second is the vector potential generated by the nuclear magnetic moment[2]:

$$A = A_0 + A_n \tag{8}$$

$$A_0 = \frac{(B \times r_0)}{2} \tag{9}$$

$$A_n = \frac{(\mu \times r_n)}{r_n^3} \tag{10}$$

where r_0 is the distance from the gauge origin to the electron and r_n is the distance from the nucleus to the electron. If we use the Coulomb gauge in which we place the gauge origin at the nucleus for which we want to calculate the shielding, we have $r_0 = r_n = r$, and we can write:

$$A = \frac{(B \times r)}{2} + \frac{(\mu \times r)}{r^3} \tag{11}$$

Following Ramsey[36], if we consider a nucleus with a magnetic moment of magnitude μ pointing in the z-direction in the presence of an external magnetic field B, also along the z-axis, the three components of the magnetic vector potential become:

$$A_x = -\frac{1}{2}By - \frac{\mu y}{r^3} \tag{12}$$

$$A_y = \frac{1}{2}Bx + \frac{\mu x}{r^3} \tag{13}$$

$$A_z = 0 \tag{14}$$

Substituting these into the Hamiltonian in the presence of a magnetic field,

$$\hat{H} = \left(\frac{1}{2m}\right)\left[\left(p_x + \frac{e}{c}A_x\right)^2 + \left(p_y + \frac{e}{c}A_y\right)^2 + \left(p_z + \frac{e}{c}A_z\right)^2\right] + V \tag{15}$$

The Hamiltonian can be separated into zeroth, first, and second-order terms:[36]

$$\hat{H} = \hat{H}^{(0)} + \hat{H}^{(1)} + \hat{H}^{(2)} \tag{16}$$

$$\hat{H}^{(0)} = -\left(\frac{\hbar^2}{2m}\right)\nabla^2 + V \tag{17}$$

$$\hat{H}^{(1)} = \left(\frac{e\hbar}{2mci}\right)\left(B + \frac{2\mu}{r^3}\right)\left(x\frac{\partial}{\partial y} - y\frac{\partial}{\partial x}\right) = \left(\frac{e}{2mc}\right)\left(B + \frac{2\mu}{r^3}\right)(L_z) \tag{18}$$

$$\hat{H}^{(2)} = \left(\frac{e^2}{8mc^2}\right)\left(B + \frac{2\mu}{r^3}\right)^2 (x^2 + y^2) \tag{19}$$

Where we have used $L_z = \frac{\hbar}{i}\left(x\frac{\partial}{\partial y} - y\frac{\partial}{\partial x}\right)$ in equation 18. Using second-order perturbation theory and assigning those terms as the second-order perturbation which are linear in both B and μ, we have:[2,36-38]

$$\sigma_{zz} = E^{(2)} = \left(\frac{e^2}{2mc^2}\right)\langle 0\left|\frac{x^2 + y^2}{r^3}\right|0\rangle + \left(\frac{e^2}{2m^2c^2}\right)\left\{\sum_{q>0}\frac{\langle q\left|\frac{L_z}{r^3}\right|0\rangle\langle 0|L_z|q\rangle + \langle q|L_z|0\rangle\langle 0\left|\frac{L_z}{r^3}\right|q\rangle}{E_q - E_0}\right\} \tag{20}$$

Or, in SI units[37]:

$$\sigma_{zz} = E^{(2)} = \left(\frac{\mu_0 e^2}{8\pi m}\right)\langle 0\left|\frac{x^2+y^2}{r^3}\right|0\rangle + \left(\frac{\mu_0 e^2}{8\pi m^2}\right)\left\{\sum_{q>0}\frac{\langle q\left|\frac{L_z}{r^3}\right|0\rangle\langle 0|L_z|q\rangle + \langle q|L_z|0\rangle\langle 0\left|\frac{L_z}{r^3}\right|q\rangle}{E_q - E_0}\right\} \quad (21)$$

The first term is called the diamagnetic correction to the energy and the second is called the paramagnetic correction.[36] The separation into diamagnetic and paramagnetic shielding is somewhat arbitrary, and neither of these terms has to do with unpaired electrons. By examining these two terms in detail, we can understand how certain trends in the magnetic shielding evolve.

Looking at the diamagnetic term, we see that the operator for this term involves the x- and y-coordinates of each electron, in addition to a $1/r^3$ dependence on the distance between the electron and the nucleus. This means that the diamagnetic shielding is related to the electron density perpendicular to the axis of the shielding and magnetic field (both z in this case) and decreases with increasing distance between the nucleus and electron density.

For hydrogen nuclei, the diamagnetic term will usually (but not always[39]) dominate the shielding, both because s-orbitals have a nonzero electron density at the nucleus and because the paramagnetic term contains angular momentum, which for s-orbitals is zero. For nuclei other than hydrogen, however, the paramagnetic term is usually larger than the diamagnetic term, which explains why ^{1}H nuclei have a relatively small chemical shift range compared to heavy nuclei containing p- and d-orbitals.

In addition to involving angular momentum, the paramagnetic term involves contributions from excited states, and is weighted by the energy difference between the ground and excited state. Therefore, the paramagnetic contribution to shielding will be larger for species that have low-lying excites states, such as ^{13}C nuclei that are involved in double or triple bonds.[40]

One difficulty in calculation of NMR shielding is the choice of gauge origin. This problem occurs because the choice of magnetic vector potential is not unique, in other words a constant Δf can be added to the magnetic vector potential giving the same result for the magnetic field:

$$B = \nabla \times A + \Delta f = \nabla \times A \quad (22)$$

A change in the definition of the magnetic vector potential A, otherwise known as a change in gauge origin, leads to additional terms in both the diamagnetic and paramagnetic shielding terms. In the limit of an infinite basis set, these terms cancel, but with a limited basis set, this cancellation will be incomplete, and the calculated shielding will depend on the choice of gauge origin. The total magnetic shielding, the sum of the diamagnetic and paramagnetic terms, is a quantum mechanical observable, so it should not depend on the choice of gauge origin.

This dependence of calculated magnetic shielding on choice of gauge origin is called the gauge origin problem. Several solutions have been proposed to solve the gauge origin problem, including the Gauge-Including Atomic Orbitals or Gauge-Invariant Atomic Orbitals (GIAO) method of Ditchfield,[41] the Individualized Gauge for Localized Orbitals (IGLO) method of Kutzelnigg,[42] the Localized Orbital Local Origin (LORG) method of Hansen and Bouman,[43] and the Continuous Set of Gauge Transformations (CSGT) method of Keith and Bader.[44,45]

1.3 Chemical Shift and Shielding

Chemical shift is an experimentally measured parameter; the corresponding quantum mechanical observable is the magnetic shielding (sometimes historically called the “chemical shielding”). The Greek letter δ is usually used to denote chemical shift, while σ is used for shielding. The chemical shift is the position of a peak in the experimental NMR spectrum (or the center of a peak multiplet in the presence of spin-spin coupling), and is referenced to an agreed-upon reference compound,

for example tetramethylsilane (TMS – 0.00 ppm) for proton and carbon chemical shifts. Shielding, on the other hand, is referenced to a bare nucleus. Chemical shift and shielding go in opposite directions, i.e. a less-shielded nucleus has a higher chemical shift, as shown in Figure 2.

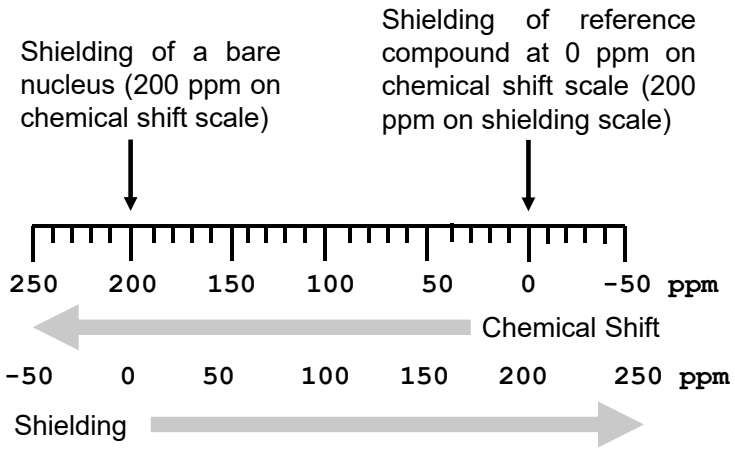

Figure 2. Difference between shielding and chemical shift.

There are several ways to convert a calculated shielding value to a chemical shift for comparison with experiment. If the absolute shielding of the nucleus in question (the shielding of the bare nucleus) is known, this absolute shielding scale can be used to convert magnetic shielding to chemical shift. Absolute shielding scales can be determined from molecular beam experiments[34], and absolute shielding scales have been reported for several nuclei.[46-58] However, many of these shielding scales were determined in the non-relativistic limit before it was determined how important relativistic corrections to shielding of even light nuclei are, and will need to be revised.[59]

The simplest way to convert a calculated magnetic shielding value into a chemical shift is to calculate the magnetic shielding of the reference compound (e.g. TMS) using the same model chemistry (level of theory and basis set) as the calculation for the nucleus of interest. The experimental chemical shift is then given by:

$$\delta_{nucl} = \sigma_{ref} - \sigma_{nucl} \tag{23}$$

where δ_{nucl} is the chemical shift of the nucleus in question, σ_{ref} is the calculated shielding of the reference compound, and σ_{nucl} is the calculated shielding of the nucleus in question. As can be seen from equation 23, any systematic error in shielding calculation will be eliminated when converting to chemical shifts, as long as the systematic error is the same in the nucleus of interest and the reference compound. Thus, an alternative way to convert between shielding and chemical shift is to use a secondary reference that is similar to the compound or set of compounds of interest, such that any systematic error in the shielding is expected to be the same in the reference and the nucleus of interest. For example, when calculating chemical shifts with respect to TMS of aromatic carbons in carbon nanotubes and fullerenes, Autschbach and coworkers found that agreement with experiment could be improved by using benzene as a secondary reference compound[60]. The shielding of benzene was calculated at the same level of theory as the compounds of interest, the calculated shielding of the nucleus of interest was subtracted from the calculated shielding of benzene, and this number was added to the experimental chemical shift of benzene relative to TMS. They found that for GIPAW calculations with the PBE functional, the difference in carbon chemical shifts calculated with the two different reference schemes was 11.1 ppm.

In a study of calculated ^{95}Mo chemical shifts in molybdenum clusters in the liquid phase, Nguyen et al.[61] found that including explicit solvent molecules in the calculation of the shielding of the reference compound, MoO_4^{2-}, in addition to the calculation of the shielding of the compounds of interest, was shown to be necessary for obtaining accurate chemical shift values.

Another method of converting calculated shielding to chemical shift involves using the slope and intercept from a graph of calculated shielding vs. experimental chemical shift for a large number of nuclei. As shown in Figure 3, the ideal slope of a graph like this is -1 and the y-intercept is the shielding of the reference compound at 0 ppm. This method is advantageous when reliable experimental chemical shifts are available for a wide variety of nuclei in compounds that are related to those that are the subject of study. When experimental gas-phase NMR data are available, these values are preferable to use since they are free from intermolecular influences of the solvent and bulk susceptibility effects. Using this method, Xin et al[62] have shown that ^{15}N shielding constants that are converted to chemical shifts in this manner can be used to confidently distinguish between regioisomers, tautomers, and protonation states of nitrogen-containing compounds. They also advocate adding an empirical correction of -16.5 ppm to calculated NH_2 nitrogen chemical shifts in order to eliminate systematic error and bring them into agreement with other nitrogen chemical shifts. Keep in mind that when using this method, the slope and intercept used for correcting the calculated chemical shifts must have been determined from the relationship between experimental chemical shifts and shielding constants calculated at the same level of theory and basis set as the current calculations.

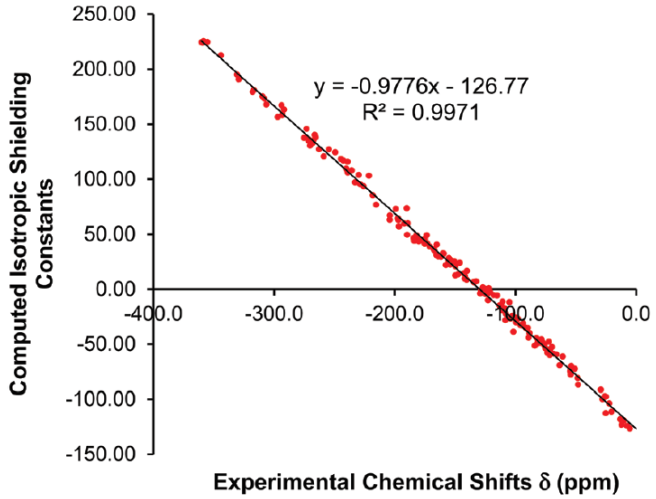

Figure 3. Calculated ^{15}N NMR shielding constant vs experimental chemical shift for a series of nitrogen-containing compounds. Reproduced from Ref. 62 with permission from The Royal Society of Chemistry.

As an alternative to converting calculated shielding values to chemical shifts for comparison with experiment, Jackowski and coworkers[63-65] recently introduced a novel method for experimentally determining magnetic shielding values. This method involves experimentally measuring the absolute resonance frequency of the nucleus of interest as well as the absolute resonance frequency of ^{2}D in a common lock solvent. The shielding of the nucleus of interest can then be determined from the known shielding constant of the deuterated solvent (several are provided in their publications) and the relative nuclear magnetic moments of deuterium and either proton or carbon (which are known to sufficient accuracy.) Using this method, shielding constants can be determined experimentally, and can then be directly compared to calculated shielding constants.

1.4. Choice of Model Chemistry

When choosing a method by which to calculate NMR shielding, which involves choosing the level of theory and basis set, one needs to consider the desired accuracy, size of the system to be investigated, and available computational resources. The accuracy of a particular method for predicting NMR shielding constants or chemical shifts can be evaluated by comparing a number of calculated chemical shifts to carefully-determined experimental values, or the calculated shielding values can be benchmarked against high-level calculations, such as CCSD(T)/cc-pVQZ.[66] Various methods have been used to assess the quality of these comparisons, including the root-mean-square (rms) error, root-mean-square percentage error, or the slope and correlation coefficient of a linear regression between calculated and experimental (or benchmark) shielding constants. Keep in mind that a small rms error or a large correlation coefficient for a set of calculated shielding constants does not necessarily guarantee accurate results for any one particular data point.

Keal and Tozer have developed a series of GGA exchange-correlation functionals that have been shown to provide highly accurate absolute NMR shielding values at a reasonable computational cost.[67-70] Specialized basis sets have also been developed that were optimized for calculating NMR shielding.[71]

Silva et al.[72] found that B3LYP/6-31G* calculated ^{13}C and ^{1}H NMR chemical shifts of a novel metabolite 4-formylaminoantipyrine were not sufficient to distinguish between two different rotamers of this compound, and instead used calculated J-coupling constants to distinguish between the two rotamers.

Amos and Kobayashi[73] explored the basis set dependence (including Jenson's specialized basis functions[71]) of calculated shielding constants within a fragment approach. They found that large basis sets, up to quadruple-zeta, were required for accurate prediction of chemical shifts, but that the fragmentation approach could reduce computational costs.

Rusakov et al.[74] explored the effect of the choice of level of theory and basis set, method for inclusion of solvent effect, vibrational and relativistic corrections on calculated ^{15}N and ^{31}P chemical shifts in solution. They found that the CCSD(T) method was preferable when computational resources allow it, but the OLYP and KT2 functionals provide similarly accurate results at the DFT level of theory. They found that relativistic corrections were negligible in the set of compounds they studied, amounting to 0.5 ppm for ^{15}N and 1-2 ppm for ^{31}P, but that solvent and vibrational effects could be on the order of 20 ppm but opposite in sign, so need to be included for accurate calculations. They recommend the aug-pcS-3/aug-pcS-2 basis sets with a locally dense basis set scheme[75,76].

2. Modeling Solvent Effects

One of the main challenges in modeling NMR chemical shifts in solution is the inclusion of solvent effects. Ideally, one would like to include all solvent molecules in the system at a quantum-mechanical level of theory. In the limit of an infinite basis set, full CI, and averaging over an *ab initio* molecular dynamics trajectory for an infinite amount of time, this would give the correct answer, but is obviously computationally intractable. The goal, therefore, is to be able to adequately predict the effect that adding a solvent would have on the resulting magnetic shielding with a reasonable computational effort. Ways of doing this include using an implicit solvent model, including a small number of explicit solvent molecules in the calculation (the "supermolecule" approach), modeling the solvent at a lower level of theory, or using a combination of the above.

Implicit solvent models are popular because they provide a way to include the ***effects*** of the solvent without modeling each individual solvent molecule, thus drastically reducing computational cost. In implicit solvent models, one molecule of the solute is placed in a cavity and the solvent is modeled as a dielectric continuum outside of this cavity. Generalized Born or Poisson-Boltzmann methods are used to describe electrostatic interactions between the solute and the solvent dielectric. Implicit solvent models have the advantage that they add minimal additional computational cost to a gas-phase calculation. Implicit models include the polarizable continuum model (PCM) of Miertuš and Tomassi,[77] or the conductor-like screening model (COSMO) of Klamt and Schüürmann.[78]

Modeling the solvent as a dielectric surrounding a cavity containing the solute incorporates long-range electrostatic effects, but necessarily neglects specific solute-solvent interactions such as hydrogen bonding. Nitrogen chemical shifts, for example, are not generally well-described using implicit solvent models due to their sensitivity to hydrogen bonding. It is therefore common to include a small number of explicit solvent molecules in a calculation with implicit solvent to account for these specific solvent-solute interactions. Including hydrogen-bonding partners, for example, has been shown to improve the accuracy of calculated ^{15}N chemical shifts[79,80]. Similarly, Sauer and coworkers found that the PCM model was not sufficient for modeling ^{17}O and ^{15}N chemical shifts in glycine, and that inclusion of explicit water molecules was necessary for accurate prediction of chemical shifts[81]. This was found to be especially true for neutral glycine, as compared to the zwitterionic form.

Semenev et al.[82] calculated ^{15}N chemical shifts in a set of heterocycles in various solvents. For nonpolar and polar aprotic solvents, using one explicit solvent molecule along with a polarizable continuum model for implicit solvent performs as well as or slightly better than the implicit solvent model alone, indicating that specific interactions between the solvent and solute do not contribute to a change in nitrogen chemical shift. On the other hand, for polar protic solvents, especially water, the use of explicit solvent molecules was recommended. For the case of pyridazine in water, the absolute error compared to experiment could be improved by addition of two and three explicit solvent molecules, as shown in Figure 4.

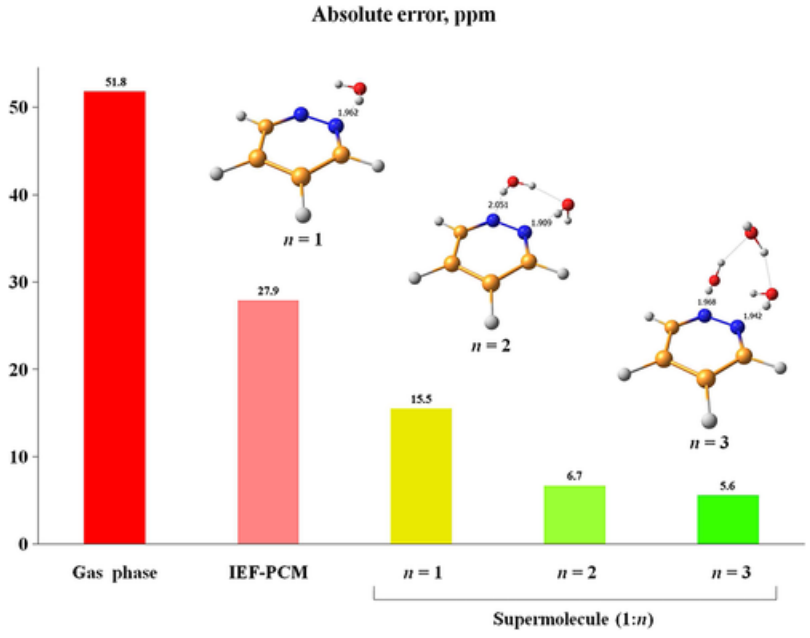

Figure 4. Decrease in absolute errors of ^{15}N NMR chemical shift of pyridazine in water when an implicit solvent model is used, and when a supermolecule model is used with increasing

numbers of explicit water molecules. Reproduced with permission of John Wiley & Sons, Ltd from V. A. Semenov, D. O. Samultsev, L. B. Krivdin, *Magn. Reson. Chem.* **2014**, *52*, 686-693.

Another option for including solvent at a reasonable computational cost is to model the solvent at a lower level of theory. The solute and hydrogen-bonding solvent molecules are modeled at a high level of theory, and the remaining solvent molecules are modeled at a less expensive level of *ab initio* or DFT method or with molecular mechanics methods. This is similar to the Quantum Mechanics/Molecular Mechanics (QM/MM) approach[83], in which the region of interest is modeled quantum-mechanically, and the rest of the molecule is included using molecular mechanics. A "locally-dense" basis set, which involves including more basis functions for the region of interest and fewer for the rest of the molecule[75], could also be used. When calculating chemical shifts for residues buried within a protein, the rest of the protein can be considered to be the "solvent." It has been shown[84,85] that modeling the residue of interest and hydrogen bonding partners explicitly and including the rest of the protein as point charges can lead to accurate chemical shifts with low computational cost. The local nature of the chemical shift facilitates the usefulness of these kinds of "hybrid" approaches.

Chemical shifts are also very sensitive to geometry. Including solvent effects during a geometry optimization is also important, in addition to including solvent effects in the chemical shift calculation. Generally, the indirect effect of solvent on shielding (the effect due to a change in molecular geometry induced by the presence of solvent[86]) is lower in magnitude than the direct solvent effect.[79] However, Roggatz et al.[87] point out that including solvent in geometry optimizations is important for stabilizing zwitterionic states - gas phase calculations can lead to a proton rearrangement to the neutral form. Thus, when considering zwitterions, including solvent in the geometry optimization is recommended.

3. Conformational Averaging

Another difficulty in modeling NMR chemical shifts is the fact that the observed chemical shift in solution will be a weighted average of the chemical shifts of all possible conformers that are present in solution during the NMR acquisition time. In order to incorporate dynamic effects into the calculation of an NMR chemical shift, what must first be known is how the chemical shift varies with molecular structure (i.e. bond lengths, dihedral angles, and other structural parameters). A plot of chemical shift (or shielding) as a function of geometric parameter(s) is known as a shielding surface. Once this shielding surface has been determined, for example by varying one geometrical parameter and calculating the shielding at each value of this parameter and fitting the results to an analytical function, the weighted average chemical shift is calculated by averaging over this shielding surface. In order to do this, the distribution of conformers in the sample must be known. There are two equivalent ways of determining how many molecules are present in each geometrical arrangement in solution at a given time. One can calculate the energy of all possible conformations and determine the prevalence of each species according to the Boltzmann distribution and the calculated energies. The alternative, equivalent method of determining the distribution of molecules among the various conformational possibilities is to take conformations from snapshots of a molecular dynamics simulation. Averaging over all possible conformations according to the Boltzmann distribution corresponds to taking an ensemble average of molecular conformations. Averaging over snapshots taken from an MD simulation corresponds to taking a time average. According to the ergodic hypothesis, in the limit of an infinitely long simulation, the time average and ensemble average should be equivalent.

Moyna and coworkers[88,89] have found that in the case of carbohydrates with many conformational degrees of freedom, a time ensemble generated by Boltzmann weighting better reproduces

experimental chemical shifts than sampling over conformations generated by molecular dynamics simulations. They attribute this discrepancy to the force fields used in the MD simulations not being of sufficient accuracy to reproduce the true molecular structures in solution.

In an extensive study of the effects of implicit vs explicit solvent model as well as conformational averaging, Exner et al.[90] explored ^{1}H, ^{13}C, and ^{15}N chemical shifts in the N-methyl acetamide and a larger peptide, the HA2 domain of hemagglutinin. As can be seen in Figure 5, $^{1}H^{N}$ chemical shifts are extremely sensitive to structure – varying by about 4 ppm depending on which snapshot of the MD simulation is chosen. The choice of explicit vs implicit solvent changes the average calculated chemical shift by about 2 ppm. In addition, the deviation of chemical shifts throughout the simulation is much larger in the model incorporating explicit solvent than the implicit solvent model, indicating that ^{1}H chemical shifts are also very sensitive to reorganization of the surrounding solvent geometry. The $^{1}H^{N}$ chemical shift was shown to be strongly correlated with the distance between the nitrogen and hydrogen bond acceptor, or the strength of the hydrogen bond. Carbon chemical shifts were found to be less sensitive to solvent effects, and for the carbonyl carbon the effects of conformational change of the molecule itself were stronger than the influence of structural fluctuations of the solvent. ^{15}N chemical shifts were shown to be the most strongly influenced by structural changes and solvent effects, with the $^{15}N^{H}$ chemical shift spanning 40 ppm in the course of the N-methyl acetamide simulation, which is on the order of the range of experimental ^{15}N chemical shifts. Last, in the MD simulation of the 32-residue peptide, as expected, $^{1}H^{N}$ chemical shifts of residues buried within the peptide and participating in intramolecular hydrogen bonds were much less sensitive to the choice of explicit or implicit solvent than $^{1}H^{N}$ chemical shifts of residues that are located on the outside of the protein, which are expected to be influenced by fluctuations in the explicit solvent structure.

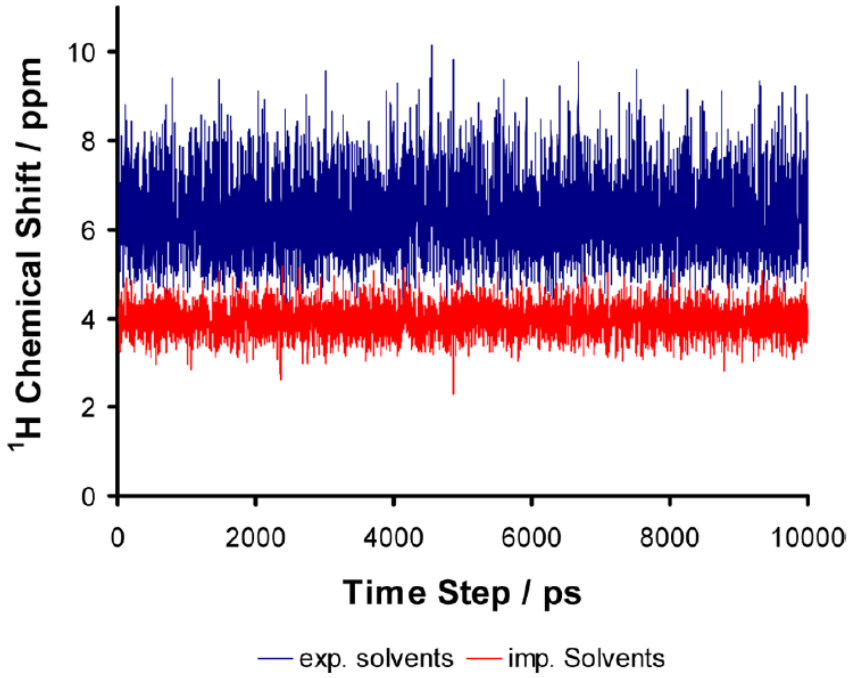

Figure 5. Time series of $^{1}H^{N}$ chemical shift of the amide group in n-methyl acetamide, calculated from snapshots taken from molecular dynamics simulations using either explicit or implicit solvent. Reprinted with permission from T. E. Exner, A. Frank, I. Onila, H. M. Möller, *J. Chem. Theory Comput.* **2012**, *8*, 4818-4827. Copyright 2012 American Chemical Society.

Mineva et al.[91] explored ^{13}C chemical shifts in two amphiphilic systems: sodium octanoate and hexadecyltetramethyl ammonium chloride. They averaged over snapshots from MD simulations performed in water, after validating that the MD simulations reproduced experimental values such as molecular surface charge from neutron diffraction experiments. Chemical shifts calculated using implicit and explicit solvent models, for both static geometry-optimized structures and averages over the MD simulations were compared. They concluded that implicit solvent does a sufficient job at reproducing ^{13}C NMR chemical shifts, especially in cases such as the large hexadecyltetramethyl ammonium chloride molecule, for which calculations with explicit solvent were too computationally demanding. As expected, the worst agreement with experiment when using the implicit solvent model is for the carboxylate carbon. Calculated chemical shift values converged very rapidly with respect to the number of MD snapshots that were sampled.

Amide proton chemical shifts in proteins are especially important, as they form the starting point for peak assignments. Zhu et al.[92] explored various factors that influence calculated amide proton chemical shifts, including choice of density functional, size of the basis set, inclusion of explicit solvent and hydrogen bonding, and the local geometry surrounding the amide proton. They used a QM/MM approach in which the molecules of interest and the buffer region were modeled quantum mechanically, and the rest of the protein was modeled using point charges. They found that including explicit solvent significantly improved agreement with experimental values over using implicit solvent, and that for accurate computations, the water molecule forming a hydrogen bond with the amide nitrogen must be modeled quantum mechanically. Results are further improved if the secondary hydrogen bond acceptor (either a water molecule or adjacent residue in the protein) is also included in the quantum mechanical region when cooperative hydrogen bonding is present. In terms of level of theory, the OPBE functional was recommended with a locally-dense basis set scheme incorporating diffuse basis functions on the nuclei of interest. Last, they found that incorporating conformational effects by averaging over molecular dynamics snapshots did not improve the agreement with experiment. The agreement could be improved with a larger number of samples, exceeding available computational resources, or a more accurate molecular mechanics force field. The authors also suggest that amide proton chemical shifts could be used as a test of potential molecular mechanics force field, due to their strong dependence on local geometry and the presence of hydrogen bonds.

Dračínský et al.[93] also encourage using predicted NMR chemical shifts as a way of evaluating new MD force fields. In their study comparing *ab initio* MD and classical MD for dynamic averaging, they found that *ab initio* MD allowed for better conformational sampling, especially for N-H distances. Using the SHAKE algorithm, which constrains X-H bonds to allow for a larger molecular dynamics time step, essentially removes the conformational sampling of these bond lengths, and instead restricts them to a very narrow set of values. Since proper conformational sampling was shown to be necessary for accurate calculation of NMR chemical shifts, even if a very high-level *ab initio* method is used for the actual NMR shielding calculation, the SHAKE algorithm should be avoided in MD simulations used to generate ensembles for shielding calculations.

To conclude this section, the reader is reminded that when calculating magnetic shielding, the choice of method to use will always be a compromise between accuracy and computational resources available. For example, the use of *ab initio* MD is not practical for large molecules of biological importance,[93] so empirical force fields must be used. In some cases, due to inaccuracies of these empirical force fields, the ability to use a higher level of theory for a calculation at one optimized geometry using implicit solvent may lead to a better agreement with experiment than a calculation that takes conformational averaging into account at a lower level of theory.

4. Other factors influencing chemical shifts

Other factors that may influence the chemical shifts of small molecules in solution include pH, temperature, and concentration. In many systems, dimerization or aggregation occurs at high concentrations, and the observed chemical shift in solution will be a weighted average of the monomer and aggregate chemical shifts. We and others have used this to our advantage to determine binding constants and gain insight into the geometry of dimers formed. Although the agreement is not perfect, calculated carbon chemical shifts were used to select among the best dimer structures for anti-malarial drugs.[94,95] Proton chemical shifts incorporating Boltzmann weighting of several low-energy conformers of naphthalenedicarboxylic acids indicated that pi-pi interactions are not important in these dimers.[96]

Flores et al.[97] explored the change in chemical shift of the hydroxyl proton of *n*-hexanol with increasing fraction of *n*-hexanol in cyclohexane. Clusters of *n*-hexanol as large as hexamers were optimized using DFT, and the respective chemical shifts were calculated. These calculated chemical shifts reproduced the experimental trend of increasing chemical shift of the hydroxyl proton with increasing *n*-hexanol mole fraction.

Relativistic corrections are important for chemical shift calculations of heavy nuclei. Rusakova et al.[98] found that solvent and rovibrational effects contributed 8 and 6%, respectively, of the total shielding in calculations of ^{125}Te chemical shifts. Relativistic effects, on the other hand, contributed 20-25%. Fukal et al.[99] determined that effects of solvent and relativistic effects were necessary to include in order to accurately predict ^{31}P chemical shifts, but that ^{31}P in phosphates and thiophosphates could be distinguished on the basis of calculated chemical shifts. Relativistic effects were also found to be significant when calculating the absolute shielding of ^{31}P using ab initio methods.[100] The reader is referred to recent reviews[3] for more detailed discussions of relativistic effects on magnetic shielding.

5. Applications

As we have mentioned in the previous sections, calculating NMR chemical shifts for solvated systems comes with a variety of difficulties. Solvent effects, conformational averaging, aggregation, changes in pH, and relativistic effects for heavy atoms must be taken into account with a reasonable computational cost. Magnetic shielding values must be converted to chemical shifts for comparison with experiment. Fortuitous error cancellation may obscure results. In the case of density functional theory, there is no way to know *a priori* whether one method is better than another. Comparing calculated shielding constants with experimental chemical shifts may lead to a low rmsd for a collection of molecules, but good statistics may hide errors for individual nuclei.

Nevertheless, several groups have shown that calculated shielding values can be compared to experimental chemical shifts to gain structural information. Touw et al.[101] used a very inexpensive calculation (B3LYP/6-31G) to calculate ^{1}H and ^{13}C chemical shifts in different conformations of retinal. They concluded that this level of theory does a reasonable job reproducing experimental ^{13}C NMR chemical shifts, with results comparable to plane-wave pseudopotential calculations. Importantly, the upfield shifts in C-12 of 13-*cis*-retinal, C-10 of 11-*cis*-retinal, and C-8 of 9-*cis*-retinal compared to the all-*trans* conformer were reproduced in the calculated shielding values. For 11-*cis*-retinal, averaging the calculated chemical shift values for the 11-*cis*-12-s-*cis* and 11-*cis*-12-s-*trans* conformations, since both are present in solution, leads to especially good agreement with the experimental chemical shift value measured in solution.

Domínguez et al.[102] were able to use calculated ^{1}H and ^{13}C chemical shifts to determine the correct diastereomer of the marine natural product okadic acid. They found that using a continuum

solvent model improved the accuracy of the calculations. Yi et al.[103] used calculated shielding values to validate peak assignments in the Chinese medicinal compound emodin. Semenov et al.[104] used the large difference in calculated ^{15}N chemical shift between amine and imine nitrogens and the accuracy of calculated ^{15}N chemical shifts, along with the experimental ^{15}N chemical shift of 4-trifluoromethyl[b]benzo-1,4-diazepine to show that this compound exists primarily in the imine form.

De Souza et al.[105] found that performing a DFT geometry optimization in the gas phase followed by NMR chemical shift calculation using the PCM model to incorporate solvent effects led to reasonable agreement with experimentally-measured NMR chemical shifts in solution for the flavenoids epigallocatechin, kaempferol and quercetin. They also showed that geometry-optimized structures could be rotated about a single dihedral angle, keeping all other parameters fixed at the optimized geometry, in order to bring the calculated NMR chemical shifts into better agreement with experiment. This indicates that the most populated dihedral angle in solution is different from the lowest-energy dihedral angle in the gas phase, and that this technique – changing one geometrical parameter to improve agreement between calculated and experimental chemical shifts – could be used as a tool for refining solution-state geometries of small molecules.

Siskos et al.[106] argue that due to their incredible sensitivity to structural parameters and interactions such as hydrogen bonds, calculated chemical shifts can lead to structural information that is of greater accuracy than that obtained by single-crystal X-ray studies.

6. Conclusions

To summarize, as computing power becomes more readily available and methods are developed to predict magnetic shielding tensors with greater accuracy, several important factors must be taken into consideration. The computational method chosen must be able to predict not only the correct magnetic shielding of the molecule in the geometry-optimized state, but must incorporate solvent effects on chemical shift as well as geometry, and conformational averaging. In most cases, limited computational resources necessitate a trade-off between the most accurate *ab initio* method, number of explicit solvent molecules included in the calculation, and the number of different conformations considered. Although a method may give a good correlation between experimental chemical shifts and calculated shielding for a large test set of molecules, the method may not perform adequately for one chemical shift of a particular nucleus. Fortuitous error cancellation can lead to difficulty interpreting results. Nonetheless, calculated chemical shifts in solution are being used to gain valuable structural information. Increasing computational power is allowing solvent effects and conformational averaging to be incorporated in NMR shielding calculations, and the calculation of correct NMR shielding constants has been proposed as a way to evaluate new molecular dynamics force fields.

Acknowledgements

We thank the NSF (CHE-1751529 and CHE-1725919) for partial support of this research. Acknowledgment is made to the Donors of the American Chemical Society Petroleum Research Fund for partial support of this research (58738-DNI6).

References

[1] A. C. de Dios, C. J. Jameson, *Annu. Rep. NMR. Spectro.* **2012**, *77*, 1-80.

[2] A. C. de Dios, *Prog. Nucl. Mag. Res. Sp.* **1996**, *29*, 229-278.

[3] C. J. Jameson, A. C. de Dios, in *Nuclear Magnetic Resonance: A Specialist Periodical Report* (Ed.: G. A. Webb), The Royal Society of Chemistry, London, **2015**, *44*, pp 46-75 (and other volumes in this series)

[4] T. Helgaker, M. Jaszunski, K. Ruud, *Chem. Rev.* **1999**, *99*, 293-352.

[5] F. A. A. Mulder, M. Filatov, *Chem. Soc. Rev.* **2010**, *39*, 578-590.

[6] A. D. Buckingham, T. Schaefer, W. G. Schneider, *J. Chem. Phys.* **1960**, *32*, 1227-1233.

[7] P. Laszlo, *Prog. Nucl. Mag. Res. Sp.* **1967**, *3*, 231-402.

[8] J. Hur, S. J. Stuart, *J. Chem. Phys.* **2012**, *137*, 054102.

[9] A. D. MacKerell, Jr., D. Bashford, M. Bellott, R. L. Dunbrack, Jr., J. D. Evanseck, M. J. Field, S. Fischer, J. Gao, H. Guo, S. Ha, D. Joseph-McCarthy, L. Kuchnir, K. Kuczera, F. T. K. Lau, C. Mattos, S. Michnick, T. Ngo, D. T. Nguyen, B. Prodhom, W. E. Reiher, III, B. Roux, M. Schlenkrich, J. C. Smith, R. Stote, J. Straub, M. Watanabe, J. Wiórkiewicz-Kuczera, D. Yin, M. Karplus, *J. Phys. Chem. B* **1998**, *102*, 3586-3616.

[10] C. C. J. Roothaan, *Rev. Mod. Phys.* **1951**, *23*, 69-89.

[11] J. B. Foresman, M. Head-Gordon, J. A. Pople, M. J. Frisch, *J. Phys. Chem.* **1992**, *96*, 135-149.

[12] R. J. Bartlett, G. D. Purvis III, *Int. J. Quantum Chem.* **1978**, *14*, 561-581.

[13] C. Møller, M. S. Plesset, *Phys. Rev.* **1934**, *46*, 618-622.

[14] P. Hohenberg, W. Kohn, *Phys. Rev*. **1964**, *136*, B864-B71.

[15] W. Kohn, L. J. Sham, *Phys. Rev.* **1965**, *140*, A1133-A38.

[16] S. H. Vosko, L. Wilk, M. Nusair, *Can. J. Phys.* **1980**, *58*, 1200-1211.

[17] J. P. Perdew in *Electronic Structure of Solids '91* (Ed.: P. Ziesche and H. Eschrig), Akademie Verlag, Berlin, **1991**, pp. 11-20.

[18] J. P. Perdew, J. A. Chevary, S. H. Vosko, K. A. Jackson, M. R. Pederson, D. J. Singh, C. Fiolhais, *Phys. Rev. B* **1992**, *46*, 6671-6687.

[19] J. P. Perdew, J. A. Chevary, S. H. Vosko, K. A. Jackson, M. R. Pederson, D. J. Singh, and C. Fiolhais, *Phys. Rev. B* **1993**, *48*, 4978.

[20] J. P. Perdew, K. Burke, and Y. Wang, *Phys. Rev. B* ***1996,*** 54*,* 16533-16539.

[21] C. Lee, W. Yang, R. G. Parr, *Phys. Rev. B* **1988**, *37*, 785-789.

[22] A. D. Becke, *Phys. Rev. A* **1988**, *38*, 3098-3100.

[23] Y. Zhao, D. G. Truhlar, *J. Chem. Phys.* **2006**, *125*, 194101.

[24] A. D. Becke, *J. Chem. Phys.* **1993**, *98*, 5648-5652.

[25] W. J. Hehre, R. F. Stewart, J. A. Pople, *J. Chem. Phys.* **1969**, *51*, 2657-2664.

[26] C. Bonhomme, C. Gervais, F. Babonneau, C. Coelho, F. Pourpoint, T. Azaïs, S. E. Ashbrook, J. M. Griffin, J. R. Yates, F. Mauri, C. J. Pickard, *Chem. Rev.* **2012**, *112*, 5733-5779.

[27] K. Ruud, P.-O. Åstrand, P. R. Taylor, *J. Chem. Phys.* **2000**, *112*, 2668-2683.

[28] K. Ruud, P.-O. Åstrand, P. R. Taylor, *J. Am. Chem. Soc.* **2001**, *123*, 4826-4833.

[29] P.-O. Åstrand, K. Ruud, *Phys. Chem. Chem. Phys.* **2003**, *5*, 5015-5020.

[30] C.J. Jameson, A. C. de Dios, in *Nuclear Magnetic Shielding and Molecular Structure* (Ed.: J. A. Tossell), Springer, Dordrecht, **1993**, pp 95-116.

[31] R. Car, M. Parrinello, *Phys. Rev. Lett.* **1985**, *55*, 2471-2474.

[32] R. Ifitmie, P. Minary, M. E. Tuckerman, *Proc. Natl. Acad. Sci. USA* **2005**, *102*, 6654-6659.

[33] J. Gauss, J. F. Stanton, *Adv. Chem. Phys.* **2002**, *123*, 355-422.

[34] K. Jackowski, M. Jaszuński, *Gas Phase NMR*, Royal Society of Chemistry Publishing, Cambridge, **2016**.

[35] M. Kaupp, M. Bühl, V. G. Malkin, *Calculation of NMR and EPR Parameters: Theory and Applications*, VCH, Weinheim, **2004**.

[36] N. F. Ramsey, *Phys. Rev.* **1950**, *78*, 699-703.

[37] G. A. Webb in *Nuclear Magnetic Shielding and Molecular Structure* (Ed.: J. A. Tossell), Springer, Dordrecht, **1993**, pp.1-25.

[38] J. C. Facelli, *Concepts Magn. Reson. A* **2004**, *20*, 42-69.

[39] P. Garbacz, V. V. Terskikh, M. J. Ferguson, G. M. Bernard, M. Kędziorek, R. E. Wasylishen, *J. Phys. Chem. A* **2014**, *118*, 1203-1212.

[40] J. Prestegard, "Origin of Chemical Shifts," can be found under http://tesla.ccrc.uga.edu/courses/BioNMR2014/lectures/pdfs/Origin_of_Chemical_Shifts_14.pdf, **2014.**

[41] R. Ditchfield, *Mol. Phys.* **1974**, *27*, 789-807.

[42] W. Kutzelnigg, *Isr. J. Chem.* **1980**, *19*, 193-200.

[43] A. E. Hansen, T. D. Bouman, *J. Chem. Phys.* **1985**, *82*, 5035-5047.

[44] T. A. Keith, R. F. W. Bader, *Chem. Phys. Lett.* **1993**, *210*, 223-231.

[45] T. A. Keith, R. F. W. Bader, *J. Chem. Phys.* **1993**, *99*, 3669-3682.

[46] G. A. Aucar, I. A. Aucar, *Annu. Rep. NMR Spectro.* **2019**, *96*, 77-141.

[47] C. J. Jameson, *Encyclopedia of Magnetic Resonance*, eds-in-chief R. K. Harris and R. E. Wasylishen, John Wiley: Chichester. DOI: 10.1002/9780470034590.emrstm0072.pub2. Published online 15 March 2011.

[48] C. J. Jameson, A. K. Jameson, P. M. Burrell, *J. Chem. Phys.* **1980**, *73*, 6013-6020.

[49] C. J. Jameson, A. K. Jameson, D. Oppusunggu, S. Wille, P. M. Burrell, J. Mason, *J. Chem. Phys.* **1981**, *74*, 81-88.

[50] C. J. Jameson, A. K. Jameson, J. Honarbakhsh, *J. Chem. Phys*. **1984**, *81*, 5266-5267.

[51] C. J. Jameson, A. K. Jameson, *Chem. Phys. Lett.* **1987**, *135*, 254-259.

[52] A. K. Jameson, C. J. Jameson, *Chem. Phys. Lett.* **1987**, *134*, 461-466.

[53] C. J. Jameson, A. K. Jameson, *Chem. Phys. Lett.* **1988**, *149*, 300-305.

[54] C. J. Jameson, A. C. de Dios, A. K. Jameson, *Chem. Phys. Lett.* **1990**, *167*, 575-582.

[55] R. E. Wasylishen, C. Connor, J. Friedrich, *Can. J. Chem.* **1984**, *62*, 981-985.

[56] A. Laaksonen, R. E. Wasylishen, *J. Am. Chem. Soc.* **1995**, *117*, 392-400.

[57] M. Gee, R. E. Wasylishen, A. Laaksonen, *J. Phys. Chem. A* **1999**, *103*, 10805-10812.

[58] R. E. Wasylishen, D. L. Bryce, *J. Chem. Phys.* **2002**, *117*, 10061-10066.

[59] A. Faucher, R. E. Wasylishen in *Gas Phase NMR* (Eds.: K. Jackowski, M. Jaszuński), Royal Society of Chemistry Publishing, Cambridge, **2016**, pp. 52-94.

[60] E. Zurek, C. J. Pickard, B. Walczak, J. Autschbach, *J. Phys. Chem. A.* **2006**, *110*, 11995-12004.

[61] T. T. Nguyen, J. Jung, X. Trivelli, J. Trébosc, S. Cordier, Y. Molard, L. Le Pollès, C. J. Pickard, J. Cuny, R. Gautier, *Inorg. Chem.* **2015**, *54*, 7673-7683.

[62] D. Xin, C. A. Sader, U. Fischer, K. Wagner, P.-J. Jones, M. Xing, K. R. Fandrick, N. C. Gonnella, *Org. Biomol. Chem.* **2017**, *15*, 928-936.

[63] K. Jackowski, M. Jaszuński, M. Wilczek, *J. Phys. Chem. A* **2010**, *114*, 2471-2475.

[64] P. Garbacz, K. Jackowski, *Chem. Phys. Lett.* **2019**, *728*, 148-152.

[65] P. Garbacz, K. Jackowski, W. Makulski, R. E. Wasylishen, *J. Phys. Chem. A* **2012**, *116*, 11896-11904.

[66] D. Flaig, M. Maurer, M. Hanni, K. Braunger, L. Kick, M. Thubauville, C. Ochsenfeld, *J. Chem. Theory Comput.* **2014**, *10*, 572-578.

[67] T. W. Keal, D. J. Tozer, *J. Chem. Phys.* **2003**, *119*, 3015-3024.

[68] M. J. Allen, T. W. Keal, D. J. Tozer, *Chem. Phys. Lett.* **2003**, *380*, 70-77.

[69] T. W. Keal, D. J. Tozer, T. Helgaker, *Chem. Phys. Lett.* **2004**, *391*, 374-379.

[70] T. W. Keal, D. J. Tozer, *J. Chem. Phys.* **2004**, *121*, 5654-5660.

[71] F. Jensen, *J. Chem. Theory Comput.* **2015**, *11*, 132−138.

[72] S. Cavalcante Silva, S. M. M. Rodrigues, V. Nardini, A. d. L. L. Vaz, V. Palaretti, G. V. J. da Silva, R. Vessecchi, G. C. Clososki, *J. Mol. Struct.* **2018**, *1163*, 280-286.

[73] R. Amos, R. Kobayashi, *J. Phys. Chem. A* **2016**, *120*, 8907-8915.

[74] Y. Yu. Rusakov, I. L. Rusakova, V. A. Semenov, D. O. Samultsev, S. V. Fedorov, L.B. Krivdin, *J. Phys. Chem. A.* **2018**, *122*, 6746-6759.

[75] D. B. Chestnut, K. D. Moore, *J. Comput. Chem.* **1989**, *10*, 648-659.

[76] D. B. Chestnut, E. F. C. Byrd, *Chem. Phys.* **1996**, *213*, 153-158.

[77] S. Miertuš, E. Scrocco, J. Tomasi, *Chem. Phys*. **1981**, *55*, 117-129.

[78] A. Klamt, G. Schüürmann, *J. Chem. Soc. Perkins Tran.* **1993**, *2*, 799-805.

[79] M. N. Manalo, A. C. de Dios, R. Cammi, *J. Phys. Chem. A* **2000**, *104*, 9600-9604.

[80] M. Witanowski, Z. Biedrzycka, W. Sicinska, Z. Grabowski, *J. Magn. Reson.* **1998**, *131*, 54-60.

[81] M. C. Caputo, P. F. Provasi, S. P. A. Sauer, *Theor. Chem. Acc.* **2018**, *137*, 88.

[82] V. A. Semenov, D. O. Samultsev, L. B. Krivdin, *Magn. Reson. Chem.* **2014**, *52*, 686-693.

[83] A. Warshel, M. Levitt, *J. Mol. Biol.* **1976**, *103*, 227-249.

[84] A. C. de Dios, J. G. Pearson, E. Oldfield, *Science* **1993**, *260*, 1491-1496.

[85] A. C. de Dios, E. Oldfield, *Chem. Phys. Lett.* **1993**, *205*, 108-116.

[86] R. Cammi, *J. Chem. Phys.* **1998**, *109*, 3185-3196.

[87] C. C. Roggatz, M. Lorch, D. M. Benoit, *J. Chem. Theory Comput.* **2018**, *14*, 2684-2695.

[88] E. P. O'Brien, G. Moyna, *Carbohyd. Res.* **2004**, *339*, 87-96.

[89] C. W. Swalina, E. P. O'Brien, G. Moyna, *Magn. Reson. Chem.* **2002**, *40*, 195-201.

[90] T. E. Exner, A. Frank, I. Onila, H. M. Möller, *J. Chem. Theory Comput.* **2012**, *8*, 4818-4827.

[91] T. Mineva, Y. Tsoneva, R. Kevorkyants, A. Goursot, *Can. J. Chem.* **2013**, *91*, 529-537.

[92] T. Zhu, J. Z. H. Zhang, X. He, *J. Chem. Theory Comput.* **2013**, *9*, 2104-2114.

[93] M. Dračinský, H. M. Möller, T. E. Exner, *J. Chem. Theory Comput.* **2013**, *9*, 3806-3815.

[94] L. B. Casabianca, A. C. de Dios, *J. Phys. Chem. A* **2004**, *108*, 8505-8513.

[95] L. B. Casabianca, A. C. de Dios, *Magn. Reson. Chem.* **2006**, *44*, 276-282.

[96] P. D. Greenstein, L. B. Casabianca, *J. Phys. Chem. B* **2017**, *121*, 5086-5093.

[97] M. E. Flores, T. Shibue, N. Sugimura, H. Nishide, I. Moreno-Villoslada, *Chem. Phys. Lett.* **2016**, *644*, 276-279.

[98] I. L. Rusakova, Y. Yu. Rusakov, L. B. Krivdin, *J. Phys. Chem. A* **2017**, *121*, 4793-4803.

[99] J. Fukal, O. Páv, M. Buděšínksý, I. Rosenberg, J. Šebera, V. Sychrovský, *Phys. Chem. Chem. Phys.* **2019**, *21*, 9924-9934.

[100] P. Lantto, K. Jackowski, W. Makulski, M. Olejniczak, M. Jaszuński, *J. Phys. Chem. A* **2011**, *115*, 10617-10623.

[101] S. I. E. Touw, H. J. M. de Groot, F. Buda, *J. Mol. Struct. – Theochem*. **2004**, *711*, 141-147.

[102] H. J. Domínguez, G. D. Crespín, A. J. Santiago-Benítez, J. A. Gavín, M. Norte, J. J. Fernández, A. Hernández Daranas, *Mar. Drugs*, **2014**, *12*, 176-192.

[103] Y. Yi, B. Adrjan, J. Wlodarz, J. Li, K. Jackowski, S. Roszak, *J. Mol. Struct.* **2018**, *1166*, 304-310.

[104] V. A. Semenov, D. O. Samultsev, A. Yu. Rulev, L. B. Krivdin, *Magn. Reson. Chem.* **2015**, *53*, 1031-1034.

[105] L. A. De Sousa, W. M.G Tavares, A. P. M. Lopes, M. M. Soeiro, W. B. De Almeida, *Chem. Phys. Lett.* **2017**, *676*, 46-52.

[106] M. G. Siskos, M. I. Choudhary, I. P. Gerothanassis, *Tetrahedron* **2018**, *74*, 4728-4737.